Journal of Peptide Science
J. Peptide Sci. **8**: 151–171 (2002)
DOI: 10.1002/psc.380

Investigation of Penetratin Peptides Part 1. The Environment Dependent Conformational Properties of Penetratin and Two of its Derivatives

ANDRÁS CZAJLIK,[a] ESZTER MESKÓ,[b] BOTOND PENKE[c] and ANDRÁS PERCZEL[a]*

[a] Department of Organic Chemistry, Eötvös University, P. O. Box 32, H-1518 Budapest 112, Hungary
[b] Department of Organic Chemistry, University of Szeged, Szeged Dóm tér 8., Hungary
[c] Department of Medical Chemistry, University of Szeged, Szeged Dugonics tér 13., Hungary

Received 23 July 2001
Revised 24 December 2001

Abstract: The homeodomain, the DNA-binding domain of Antennapedia homeoprotein, is composed of three α-helices and one β-turn between helices II and III. Its third helix from the *N*-terminal (helix III) can translocate through the cell membrane into the nucleus and can be used as an intracellular vehicle for the delivery of oligopeptides and oligonucleotides. To the best of our knowledge, this helix III, called penetratin, which consists of 16 amino acids, is internalized by cells in a specific, non-receptor-mediated manner. For a better understanding of the mechanism of the transfer, the structure of penetratin was examined in both extracellular matrix-mimetic and membrane-mimetic environments; ^{1}H-NMR and CD spectroscopic measurements were performed in mixtures of TFE/water with different ratios. The molecular conformations of two analogue peptides [(6,14-Phe)-penetratin and a 12 amino acid penetratin derivative (peptide 3)] were also studied. An atomic level comprehensive analysis of penetratin and its two analogues was performed. In a membrane-mimetic solvent system ($TFEd_2$/water = 9 : 1), on the basis of 553 distance restraints, the 4–12 region of penetratin exhibits a bent, irregular helical structure on NMR examination. Interactions between hydrophobic amino acid residues in conjunction with H-bonds stabilize the secondary structure of the molecule. Thus, both derivatives adopt a helix-like conformation. However, while (6,14-Phe)-penetratin displays both α-helical and 3_{10}-helical features, the structure of peptide 3 is predominantly a 3_{10}-helix. Of the three peptides, surprisingly (6,14-Phe)-penetratin has the largest helical content. An increase in the polarity of the molecular environment gradually disintegrates these helix-like secondary structures. In a highly aqueous molecular system ($TFEd_2$/water = 1 : 9), the fast exchange of multiple conformers leads to too few distance restraints being extracted, therefore the NMR structures can no longer be determined. The NMR data show that only short-range order can be traced in these peptides. Under these conditions, the molecules adopt nascent helix-like structures. On the other hand, CD spectra could be recorded at any TFE/water ratio and the conformational interconversion could therefore be monitored as a function of the polarity of the molecular environment. The CD data were analysed comprehensively by the quantitative deconvolution method (CCA+). All three penetratin peptides display helical conformational features in a low dielectric medium, with significant differences as a function of their amino acid composition. However, these conformational features are gradually lost during the shift from an apolar to a polar molecular environment.

Keywords: NMR; CD; penetratin; $TFEd_2$/water mixtures; helical structure; conformational ensemble

Abbreviations: FACS, fluorescence-activated cell sorter; FITC, fluorescence isothiocyanate; MBHA, p. methyl benzhydrilamine; TFE, trifluoroethanol

*Correspondence to: Dr A. Perczel Department of Organic Chemistry, Eötvös University, PO Box 32, H-1518 Budapest 112, Hungary; e-mail: perczel@para.chem.elte.hu
Contract/grant sponsor: Hungarian Scientific Research Fund; Contract/grant numbers: OTKA T030841, OTKA T032486; AKP 98-89 2,4.

INTRODUCTION

Homeodomain proteins (homeoproteins) belong to a class of trans-activating factors [1], found in most eukaryotes. They play important roles in several essential biological processes that occur primarily, but not exclusively, during periods of growth. Homeoproteins bind to specific sites in the large groove of double-stranded DNA through their homeodomains, consisting of a specific sequence of 60 amino acids. The structures and amino acid sequences of the homeodomains are highly conserved and rather similar in different species. They are structured from three α-helices interconnected by a β-turn between helices II and III [2–4]. The homeodomains are examined widely, as they provide key information on protein–DNA interactions. Investigation of the Antennapedia homeodomain, a *Drosophila* transcription factor, revealed that the third helix from the *N*-terminal, called penetratin, is responsible for the translocation across the cell membrane into the nucleus [5]. It has also been shown that the synthetic peptide corresponding to the amino acid sequence of this third helix possesses translocation properties similar to those of the entire homeodomain [6]. While this mechanism is largely unknown at present, it is believed to be a non-receptor-mediated process [7, 8].

An understanding of the molecular details of translocation is of considerable importance, since penetratin could be used as a vector to address covalently linked oligonucleotides and oligopeptides inside living cells [9,10]. Penetratin has been proposed as a universal intracellular delivery vehicle [11]. A comprehensive analysis leads to the conclusion that all three aromatic residues, both tryptophans (48 and 56) and phenylalanine (49), play crucial roles in the process of penetration [6] (the sequence positions of these residues are shown in Scheme 1). Furthermore, glutamine in position 50 is replaced by proline, but the effect of penetration remains [7], suggesting that the helical structure is perhaps not mandatory in the process of translocation. On the basis of the NMR data, Berlose *et al.* [12] proposed a preliminary solution structure of penetratin and one of its analogues.

In order to examine the structural consequence induced by mutation, we have replaced both tryptophans in penetratin, which are claimed to be important for biological success [6], with phenylalanine, (peptide 2; (6,14-Phe)-penetratin). A third, shorter, biologically effective peptide (peptide 3) was also designed, in which two pairs of residues (Q^{50}–N^{51} and R^{53}–M^{54}) were simultaneously removed from the central turn of the helix. Both deletions can be rationalized by maintaining the helical structure and the relatively high ratio of basic amino acids. CD and ^{1}H NMR spectroscopic studies were undertaken on the following molecules: penetratin, (6,14-Phe)-penetratin and a 12 amino acid penetratin derivative (labelled above as peptide 3) (Scheme 1) carried out in water and water/TFE solvent mixtures. In bioassay performed with different cell lines penetratin and the two analogues showed good membrane translocational properties although with some quantitative differences. Detailed description of the bioassay will be published in Part 2. In the present paper, comparison of the structures of these three peptides at an atomic level is reported [RCSB PDB ids 1kz0, 1kz2 and 1kz5 for penetratin, (6,14-Phe)-penetratin and Peptide 3, respectively], with a complementary study on peptide 'flexibility' as a function of the molecular environment [13].

Sequence of penetratin (Peptide 1)

1 5 10 15
43 47 52 57
R - Q - I - K - I - W - F - Q - N - R - R - M - K - W - K - K

Sequence of (6,14-Phe)-penetratin (Peptide 2)

1 5 10 15
43 47 52 57
R - Q - I - K - I - **F** - F - Q - N - R - R - M - K - **F** - K - K

Sequence of the 12 amino acid penetratin derivative (Peptide 3)

1 5 10 15
43 47 52 57
R - Q - I - K - I - W - F [Ø - Ø] R [Ø - Ø] K - W - K - K

Scheme 1 The sequence of penetratin (1–16) corresponds to the sequence of the third helix of the Antennapedia homeodomain (43–58).

METHODS

Peptide Synthesis

Peptides were synthesized in solid-phase on MBHA-resin using Boc-chemistry. Details will be published in Part 2.

^{1}H-NMR Experiments, Resonance and Sequential Assignment, Determination of Constraints and Structure Calculation

Typically, a milligram of peptide was dissolved in a mixture of D_2O and trifluoro-ethanol ($TFEd_2$ was

purchased from Cambridge Isotope) and placed in a high-quality NMR glass tube. NMR spectra were typically recorded at 500 MHz (Bruker instrument) and were processed with the InsightII-Felix97 software package. For 2D measurements, 2048 complex data points were usually acquired in the direct dimension, typically with 512 increments. Data were zerofilled up to 4 K and processed with a Kaiser window function along t_2 and with a sine-bell function (shifted 80°) over all points in the t_1 dimension. Structure determination was performed in $TFEd_2$/water = 9 : 1. Spin systems were identified by means of direct and relayed through-bond connectivities, by means of the homonuclear COSY and TOCSY spectra. In order to map through-bond connectivities, three TOCSY spectra were recorded for each molecule with the following different spin-locking times: 40, 70 and 85 ms at 298 K. The side-chain amide proton resonances of asparagine and glutamine were assigned by using intraresidual NOEs. Assignments of all protons are reported in Tables 1–4. [BMRB accession number 5289, 5290 and 5291 for penetratin, (6,14-Phe)-penetratin and Peptide 3, respectively]. Chemical shifts were referenced relative to trifluoro-ethanol (3.88 ppm) and water (4.70 ppm). No significant changes in the chemical shifts of the side-chain protons were observed for the homologous residues. Sequence-specific NMR backbone assignments were made on the basis of sequential nuclear Overhauser effects interconnecting $H^{\alpha}(i)$ and NH($i+1$), established with 2D NOE spectroscopy (NOESY). NOESY spectra were recorded at two different temperatures (288 K and 298 K) and the two different mixing times of 125 and 250 ms, respectively. Although certain of the $H^{\alpha}(n)$-NH($n+1$) correlations in the NOESY spectra were identified with some ambiguity, the sequential assignment was completed by using additional types of resonances. For all three peptides, almost all protons were successfully assigned in the system $TFEd_2$/water = 9 : 1. In contrast, in the $TFEd_2$/water = 1 : 9 solvent mixture, the spin systems could be only partly identified because of the lack of some δ and ε protons. Possibly in consequence of the internal motion of the aromatic rings in (6, 10-Phe)-penetratin, we achieved only

Table 1 ^{1}H Chemical Shift of Penetratin Obtained from the NMR Spectra Recorded in $TFEd_2$/water = 9 : 1 System at 298 K

	NH	Hα	Hβ	Hγ	Hδ	Hε	Others
Arg	—	4.10	2.03	1.75	3.15		NHδ 7.16
Gln	8.80	4.40	2.16, 2.04	2.41			NH_2 7.06, 6.27
Ile	7.80	4.08	1.94	CH_3 0.96	0.90		
				CH_2 1.55, 1.25			
Lys	7.92	4.22	1.87, 1.83	1.59, 1.48	1.74	3.01	
Ile	7.46	3.92	1.94	CH_3 0.91	0.90		
				CH_2 1.57, 1.23			
Trp	7.81	4.42	3.42, 3.31				Hε3:7.42, Hζ3:7.18, Hη2:7.05, Hζ2:7.42 NH:9.52, Hδ1:7.06
Phe	8.20	4.21	3.18				Hδ:7.26, Hε:7.34, Hζ:7.29
Gln	8.24	4.11	2.25, 2.17	2.48			NH_2 6.98, 6.29
Asn	8.22	4.48	2.89, 2.75				NH_2 7.25, 6.34
Arg	7.93	3.97	1.77, 1.69	1.48	2.85		NHδ 6.90
Arg	7.97	4.06	1.88, 1.82	1.68, 1.60	3.12		NHδ 7.03
Met	7.93	4.30	2.14, 2.09	2.69, 2.58			SCH_3 2.49
Lys	7.77	4.11	1.82	1.41, 1.33	1.62	2.92	NHε 7.45
Trp	7.78	4.56	3.39, 3.32				Hε3:7.61, Hζ3:7.12, Hη2:7.21, Hζ2:7.44 NH:9.50, Hδ1:7.21
Lys	7.72	4.13	1.84, 1.75	1.35	1.67	2.97	
Lys	7.71	4.27	1.88, 1.77	1.49, 1.44	1.70	2.99	NHε 7.46

Chemical shifts were referenced relative to $TFEd_2OH$ (3.88 ppm).

Table 2 ^{1}H Chemical Shift of Penetratin Obtained from the NMR Spectra Recorded in $TFEd_2$/water = 1 : 9 System at 298 K

	NH	Hα	Hβ	Hγ	Hδ	Hε	Others
Arg	7.62	3.97	1.85, 1.84	1.54	3.12		NHδ7.11
Gln	8.75	4.36	1.96, 1.90	2.26			(NH_2 ?)
Ile	8.32	4.09	1.74	CH_3 0.74 CH_2 1.37, 1.10	0.75		
Lys	8.23	4.17	1.54	1.18, 1.10	1.47	2.71	(NHε 7.38?)
Ile	7.96	4.02	1.64	CH_3 0.64 CH_2 1.29, 1.03	0.72		
Trp	8.03	4.52	3.10, 3.07				NH:10.04, Hδ1:7.47 (7.07?)
Phe	7.81	4.38	2.91, 2.82				(Hδ:7.06?)
Gln	8.05	4.04	1.92, 1.82	2.15			(NH_2 ?)
Asn	8.24	4.52	2.77, 2.68				$NH_2$7.52, 6.82
Arg	8.13	4.15	1.74, 1.64	1.55, 1.47	3.04		NHδ 7.08
Arg	8.12	4.15	1.76, 1.65	1.50, (1.47?)	3.01		NHδ 7.04
Met	8.05	4.29	1.84, (1.80?)	2.42, 2.38			(SCH_3 ?)
Lys	8.07	4.14	1.62, 1.55	1.23, (1.18?)	(1.57?)	(2.87?)	(NHε?)
Trp	7.93	4.57	3.21, 3.14				NH:10.04, Hδ1:7.40 (7.15, 7.52?)
Lys	7.89	4.12	1.65	1.18	1.53	2.86	NHε 7.43
Lys	8.01	4.04	1.68, 1.60	1.34	1.63	2.89	(NHε 7.24?)

Chemical shifts were referenced relative to H_2O (4.70 ppm).

Table 3 ^{1}H Chemical Shift of (6,14-Phe)-penetratin Obtained from the NMR Spectra Recorded in $TFEd_2$/water = 9 : 1 System at 298 K

	NH	Hα	Hβ	Hγ	Hδ	Hϵ	Others
Arg	—	4.04	2.16, 2.08	1.83	3.23		NHδ:720, (Hη:6.52)
Gln	9.08	4.20	2.19, 2.05	2.54, 2.44			NH_2 6.91, 6.06
Ile	7.40	4.02	1.96	CH_3 0.94 CH_2 1.55, 1.24	0.94		
Lys	7.58	4.16	1.93	1.78	1.62, 1.52	3.04	
Ile	7.39	3.83	1.96	CH_3 0.91 CH_2 1.60, 1.23	0.94		
Phe	7.77	4.33	3.21				Hδ:7.04, Hϵ:7.22,
Phe	8.33	4.28	3.25				Hδ:7.30
Gln	8.59	4.14	2.34, 2.20	2.52			NH_2 6.79, 6.04
Asn	8.33	4.42	2.97, 2.71				NH_2 7.21, 6.14
Arg	8.02	3.96	1.86	1.65, 1.57	2.98		NHδ:6.78, (Hη:6.24)
Arg	8.19	4.03	1.90, 1.78	1.62	3.15, 3.09		NHδ:6.86, (Hη:6.41)
Met	8.10	4.25	2.22, 2.17	2.77, 2.59			SCH_3 2.08
Lys	7.92	4.02	1.81, 1.76	1.44, 1.25	1.60	2.94	NHϵ 7.29
Phe	7.94	4.48	3.24, 3.10				Hδ:7.27
Lys	7.85	4.12	1.95	1.48	1.73	3.06	NHϵ 7.26
Lys	7.72	4.35	1.93, 1.82	1.49	1.72	3.04	

Chemical shifts were referenced relative to $TFEd_2OH$ (3.88 ppm).

Table 4 ^{1}H Chemical Shift of Peptide 3 Obtained from the NMR Spectra Recorded in $TFEd_2$/water = 9 : 1 System at 298 K

	NH	Hα	Hβ	Hγ	Hδ	Hε	Others
Arg	—	4.03	2.11, 2.03	1.78	3.14		NHδ 7.09
Gln	8.88	4.28	2.19, 2.06	2.52, 2.44			NH_2 6.84, 6.02
Ile	7.43	4.06	1.93	CH_3 0.91 CH_2 1.58, 1.27	0.91		
Lys	7.60	4.16	1.87	1.61, 1.49	1.77	3.04	
Ile	7.37	3.86	2.00	CH_3 0.92 CH_2 1.62, 1.24	0.94		
Trp	7.81	4.34	3.39, 3.31				Hε3:7.50, Hζ3:7.08, Hη2:7.13, Hζ2:7.08 NH:9.04, Hδ1:6.94
Phe	8.29	4.23	3.25, 3.19				Hδ:7.29, Hε:7.38, Hζ:7.34
Arg	7.86	4.04	1.98, 1.88	1.74	3.25, 3.19		NHδ 6.97
Lys	7.94	4.00	1.78, 1.70	1.26, 1.17	1.49	2.79	
Trp	7.89	4.48	3.14, 2.89				Hε3:7.50, Hζ3:7.10, Hη2:7.21, Hζ2:7.37 NH:8.60, Hδ 1:6.82
Lys	7.79	4.02	1.75	1.65	1.31	2.93	NHε 7.12
Lys	7.43	4.06	1.84	1.42, 1.38	1.65	2.95	

Chemical shifts were referenced relative to $TFEd_2OH$ (3.88 ppm).

partial assignment of the aromatic protons. In the NOESY spectra of penetratin, recorded in the system $TFEd_2$/water = 1 : 9, we were able to find only intraresidual and sequential homonuclear information. In the latter solvent mixture, the absence of medium and long-range NOEs meant that the structure of the molecule could not be determined. From spectral data obtained in $TFEd_2$/water = 9 : 1 for penetratin, (6,10-Phe)-penetratin and peptide 3, a total of 553, 410 and 291 distance constraints, respectively, were extracted. Constraints were classified into three distance ranges of 0.18–0.25 nm, 0.25–0.35 nm and 0.35–0.50 nm, corresponding to strong, medium and weak NOEs. On the basis of the molecular topology the same set of constraints were grouped into intraresidual, sequential (form i to $(i+1)$) and medium-range (form i to $(i+n)$ and $n \geq 2$) NOEs, reported in Table 5. The restraints are evenly spread along the sequence, except for the first and last amino acid residues. Structures were calculated by *ab initio* simulated annealing from a template structure. A standard protocol of the X-PLOR (3.851) program was used [14–16]. Extended conformations with correct covalent structures and bonds (no non-bonded contacts) were generated as template (input) structures. The X-PLOR topology file (topparhdg.pro) determines the geometries, *Van der Waals* radii, bond lengths, chirality for all atoms and bonds in the protein and the parameters file (parallhdg.pro) defines the force constants and other parameters used in the structure calculations. All restraints were read in the beginning of the program. During simulation starting structures were heated to a temperature of 1000 K and 30 ps of high temperature dynamic was accomplished in 6000 steps. In the first 20 ps the *Van der Waals* (repel) function was switched off, the weights of geometric and experimental constraints were set to a low value, atoms were able to move close together or through each other. In the last 10 ps of high temperature dynamics the weights of geometric parameters and the distance restraints gradually increased. Finally, the structures were cooled during a 15 ps (3000 steps) of dynamics and the value for the repel function was stepwise raised. All structures were energy minimized under a 'full-force-field' incorporating a *Van der Waals* function during this procedure. In total 50 structures were calculated arising from the starting (template) structures. Most conformers satisfy the restraints derived from the experimental data and have a good covalent geometry. For each peptide, the best

Table 5 Number and Type of Distance Restraints per Residue Assigned in Penetratin and in its Two Derivatives

Amino acid no	Penetratin			(6,14-PHE)-penetratin			Peptide 3		
	Total[a]	Sequential[b]	Medium[c]	Total	Sequential	Medium	Total	Sequential	Medium
1	14	4	0	14	3	0	11	1	0
2	34	13	5	33	11	9	31	8	1
3	42	16	12	23	9	2	32	12	7
4	35	16	7	24	6	12	27	10	3
5	40	14	16	31	9	13	23	9	1
6	54	18	20	17	8	6	42	9	9
7	36	19	10	15	2	10	25	11	6
8	38	10	11	43	7	26			
9	44	10	21	22	9	6			
10	36	12	8	30	8	11	32	8	2
11	42	10	15	41	14	12			
12	26	9	7	41	18	11			
13	32	8	6	25	7	6	32	10	5
14	38	17	6	18	6	6	35	13	3
15	31	16	0	18	9	5	18	7	1
16	11	2	1	15	3	3	13	4	0
Grand total/sequence	553	196	145	410	129	138	291	102	38

Distance-type constraints were obtained from the 2D NOESY spectra recorded in $TFEd_2$/water = 9 : 1 systems at 298 K.
[a] Total number of restraints for residue *i*.
[b] Number of neighbouring (i, $i + 1$) restraints for residue *i*.
[c] Number of medium distance restraints for residue.

structures belong to a single conformer-family. The program MOLMOL was used for RMSD calculations [17].

Consistency Checking of the Structure of Penetratin

The surprisingly low RMSD of the final structures (0.07 ± 0.03 Å) induced us to investigate the effect of the redundancy of distance restraints. Thus, we gradually removed 5%, 10%, 15%, 25% and 35% of the distance restraints from the complete list, in a random fashion. These lists, containing a significantly reduced number of restraints, were used to perform NMR-structure calculations as described earlier. For a given level of reduction, 10 different lists of restraints were generated and all were used independently to compute 50 structures. The 25 lowest energy structures from one run were selected and utilized for RMSD calculations with the program MOLMOL [17]. The averages of the RMSD values with standard deviations indicative of the given number of restraints used are reported in Table 6. On the removal of 10% of the restraints from the original list of NOEs, the RMSD value barely changed (Table 6). The elimination of additional restraints (15%, 25% and finally 35% of the complete list) resulted in a perceptible, but still small, increase of the backbone RMSD value of 0.68 ± 0.26 Å. Similar RMSD increases, as a function of the number of restraints, were obtained (not shown) for the other two penetratin derivatives, when only the relevant helical parts were compared. This indicates that the helical segments of these peptides are very well defined.

Circular Dichroism Experiments and Quantitative Spectra Deconvolution

CD spectra were recorded on a Jobin Yvon dichrograph Mark VI. Typically, three scans were acquired with a cell path length of 0.02 cm, between 185 and 280 nm. NMR-grade TFE (Aldrich) was used. Peptide concentrations of samples were 0.1–0.5 mg/ml. CD data were analysed via the recently updated version of Convex Constraint Analysis Plus (CCA+) [18,19] (I. Jákli and A. Perczel, unpublished results).

Table 6 Backbone RMSD Values of Penetratin, as Function of the Number of NOE Restraints

Residual restraints (%)	Lowest RMSD value (25 structures)	Highest RMSD value (25 structures)
100[a]	0.07 ± 0.04 Å	—
95	0.09 ± 0.04 Å	0.34 ± 0.30 Å
90	0.09 ± 0.05 Å	0.24 ± 0.26 Å
85	0.15 ± 0.07 Å	0.39 ± 0.31 Å
75	0.38 ± 0.20 Å	0.60 ± 0.39 Å
65	0.44 ± 0.34 Å	0.68 ± 0.26 Å

[a] In a systematic manner 5%, 10%, 15%, 25% and 35% of the total number of distance restraints were removed. In each run the omitted restraints were eliminated in a random mode, repeated 10 successive times. In all cases 50 structures were calculated from where 25 structures of the lowest energy were chosen. RMSD values were calculated for the backbone atoms by means of MOLMOL programme.

RESULTS

Structures of the Peptides in Highly Aqueous Medium

The preliminary CD results demonstrate that, even in aqueous solution, penetratin has a considerable population of non-random structures (~40%). (For more detailed CD analysis see below.) The NOESY spectra of the molecule contain extended series of relatively strong NH(i)/NH($i+1$) and CHβ(i)/NH($i+1$) NOEs, indicating a threshold population with ordered structures. In the central part of penetratin, a CHα(i)/NH($i+2$) NOE connectivity was also found. Locally ordered structural segments are present in the molecule and short-range order can be traced; the peptide assumes a nascent helical conformation [20]. Both long-range and medium-range NOEs, as typically observed for highly ordered structures, were absent. Further evidence for the nascent helix was derived from the significant upfield shifts of the Hα protons (except those of the two Ile) compared with the random-coil values [21,22] (Figure 1). The CD data on the two analogues furnished similar results. Although NMR spectra of the derivatives were also recorded, full spectral assignment was not performed, due to the insufficient number of the NOEs (sequential and medium range) showed that the molecules exhibit multiple structures unresolved at the NMR-timescale. This conclusion is definitely supported by CD data.

Structures of the Peptides in a Low Dielectric Environment

Structure of penetratin (peptide 1). The geometry of penetratin involves a helix-like structure in the 4–12 region, which begins and ends with a β-turn. The stretches of CHα(i)/CHβ($i+3$) and CHα(i)/NH($i+3$) also suggest that the helix starts at Lys4 and extends to Lys13. The CHα(i)/NH($i+1$) NOEs are relatively weak, but the NH(i)/NH($i+1$) NOEs are relatively strong, supporting the helical conformation [23] (Figure 2). However, this region appears to be a non-ideal α-helix. The presence of CHα(i)/NH($i+4$) and CHα(i)/NH($i+2$)-type NOEs compiled with J-coupling data, suggest both α-helical and 3_{10}-helical fragments in this region. It seems that in a hydrophobic environment this peptide adopts an irregular amphipatic helix-like structure. The aromatic rings of the tryptophan and phenylalanine in positions 6 and 7, which have been reported to play important roles in the translocation, are close to each other (Figure 3). The latter residues, with the two Ile in positions 3 and 5, form a hydrophobic core. The molecule is stabilized by interactions between the hydrophobic amino acids and by multiple hydrogen bonds, of either (i,$i+3$): [CO(Ile5)-NH(Gln8), CO(Trp6)-NH(Asn9), CO(Arg10)-NH(Lys13), CO(Arg11)-NH(Trp14)] or (i,$i+4$) type: [CO(Phe7)-NH(Arg11), CO(Gln8)-NH(Met12)]. Among the calculated 50 structures, 26 belong in the dominant conformer family. The average RMSD in atomic positions, calculated between these structures for residues 2–15, is 0.07 ± 0.04 Å for the backbone and 0.39 ± 0.11 Å for all heavy atoms.

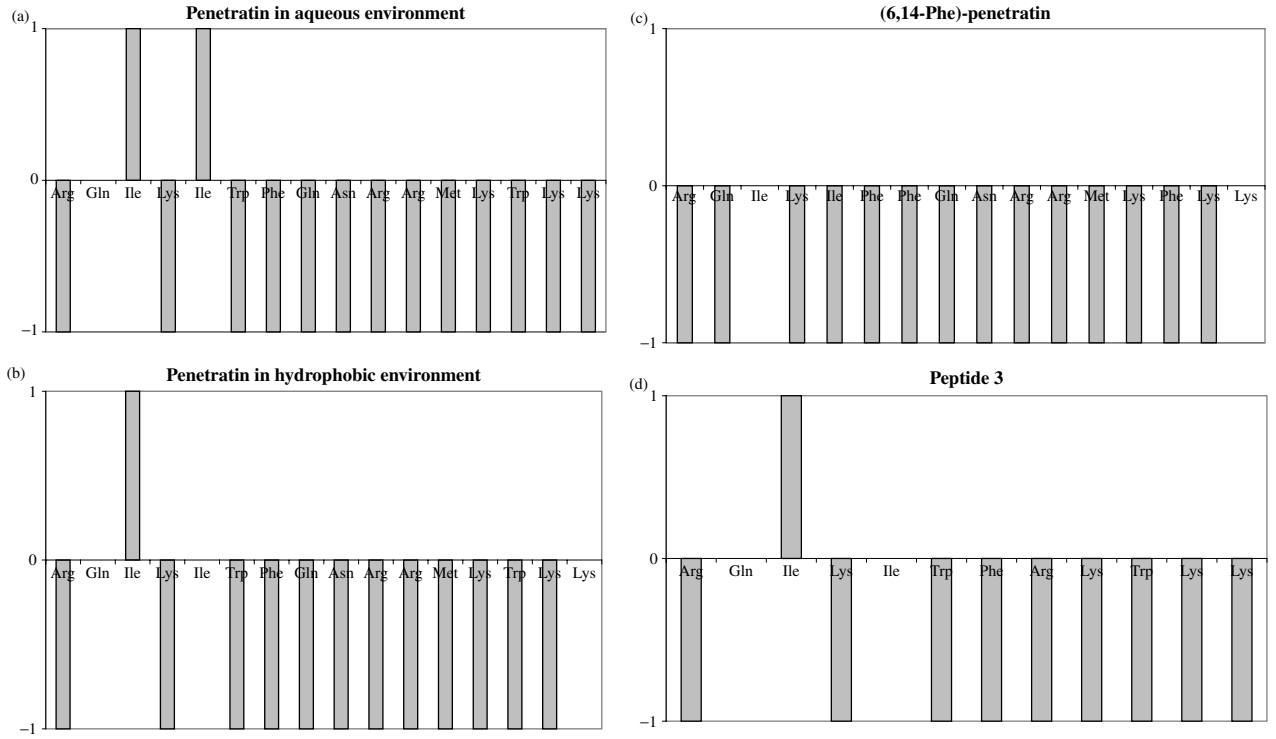

Figure 1 (a–d) H^{α} chemical shift indexes calculated from data in Tables 1–4 and random coil values [22,23]. [a]: penetratin in aqueous environment (TFE/water = 1 : 9), [b]: penetratin in hydrophobic environment (TFE/water = 9 : 1), [c]: (6,14-Phe)-penetratin (TFE/water = 9 : 1), [d]: peptide 3 (TFE/water = 9 : 1).

The comparison of the mean structure of penetratin and the third helix of the Antennapedia homeodomain [2] results as follows: the third helix of Antennapedia homeodomain consists of an 11 amino acid α-helix, followed by a random structure in the 12–16 region at the *C*-terminus of the peptide chain. The 11 amino acids of the *N*-terminal form a nearly ideal helical conformation. In contrast with penetratin, a hydrophobic core can not be found in the third helix of the Antennapedia homeodomain, the aromatic rings of tryptophan and phenylalanine in positions 6 and 7 do not interact with each other. As mentioned above, penetratin can only be described in a hydrophobic environment by one well-defined conformation; in this case the molecule has a bent helical structure in the 4–12 region (Table 8).

As mentioned earlier, Berlose *et al.* [12] described the solution structure of [biotinyl-δ-Ape-Arg1]-penetratin and one of its analogues in SDS micelles and in perfluoro-tert-butanol. The structure of penetratin determined in trifluoroethanol is similar to that found as 'A' conformer. However, in trifluoroethanol penetratin adopts a single well-defined conformation (no 'B' form could be traced). Our data show that penetratin is a non-ideal helix which looks like a 3_{10}-helix with β-turns at the two ends. Thus, penetratin in TFE shows signs of a hydrophobic core.

Structure of (6,14-Phe)-penetratin (peptide 2). This molecule adopts a helical structure, interrupted by a β-turn (Figure 4). As described later, both the 3–9 and 12–14 regions display helical properties on the basis of the dihedral angles. Thus, CHα(i)/CHβ($i+3$) and CHα(i)/NH($i+3$) NOEs, characteristic of a helical structure, can be found only in these sequential regions. In the presence of CHα(i)/NH($i+4$) and CHα(i)/NH($i+2$) NOEs, it seems that both α- and 3_{10}-helical conformations are possible. In contrast with penetratin, the aromatic rings of the phenylalanines in positions 6 and 7 do not interact with each other (Figure 4a, c). Thus, no hydrophobic core is observed for this peptide. The *N*-terminal part of the peptide has (i,$i+4$) type hydrogen bonds: CO(Gln2)-NH(Phe6), CO(Ile3)-NH(Phe7), CO(Lys4)-NH(Gln8) and CO(Ile5)-NH(Asn9), characteristic of an α-helix. The *C*-terminal half of the molecule contains three hydrogen bonds of (i,$i+3$) type: CO(Phe7)-NH(Arg10), CO(Gln8)-NH(Arg11), CO(Arg11)-NH(Phe14) and one hydrogen bond of

(a)

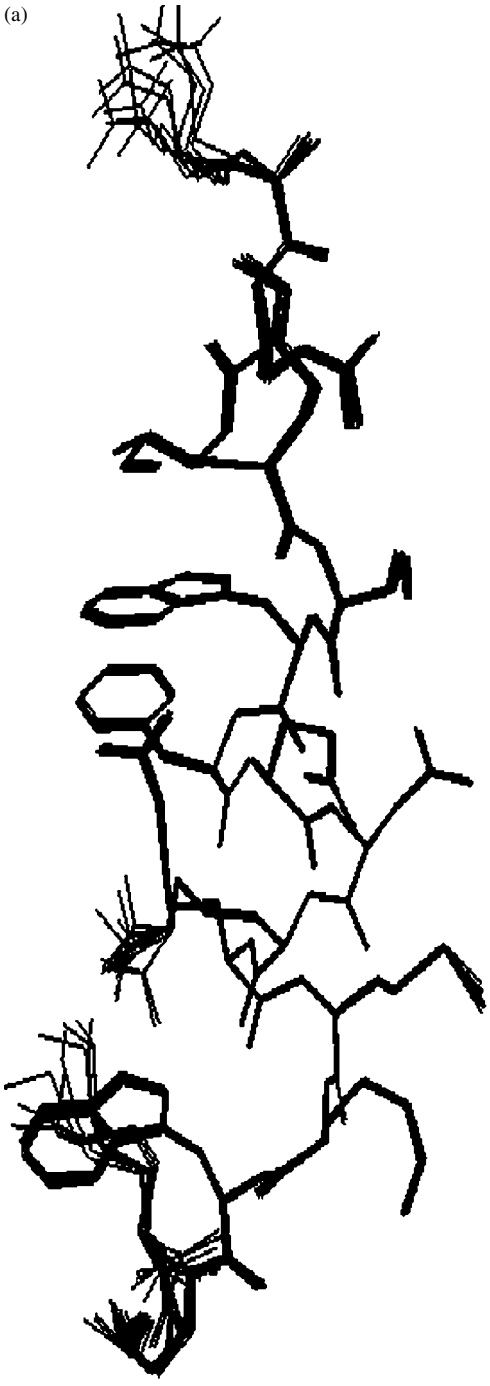

Figure 2 (a) The best 10 structures of penetratin, superimposed on the heavy atoms of residues 1–16 in TFE/water = 9 : 1 system.

$(i,i+4)$ type: CO(Met12)-NH(Lys16). These hydrogen bonds suggest a rather helical secondary structure for (6,14-Phe)-penetratin with a possible β-turn or kink in its central part. Of the calculated 50 structures, 39 belong in the dominant conformer family. When these structures were matched (residues from 2 to 15 were considered), the RMSD was 0.24 ± 0.10 Å for the backbone and 1.28 ± 0.30 Å for all heavy atoms. Comparison of the RMSD data with that of penetratin, indicated that, in contrast with penetratin, the side-chains of (6,14-Phe)-penetratin rotate without considerable restriction. This might explain the partial assignment of the aromatic protons.

Structure of peptide 3. Only the central region of this peptide exhibits a helical conformation. The dihedral angle data suggest the presence of a helical structure only in the 5–9 region (Figure 5). Examination of the stretches of CH$\alpha(i)$/CH$\beta(i+3)$ and CH$\alpha(i)$/NH$(i+3)$ led to the same conclusion. The CH$\alpha(i)$/NH$(i+2)$ NOE patterns and the disappearance of CH$\alpha(i)$/NH$(i+4)$ NOEs, suggested the presence of a 3_{10}-, rather than an α-helical conformation. Similarly as for (6,14-Phe)-penetratin, we did not find an interaction between the aromatic rings of tryptophan and phenylalanine in positions 6 and 7 (Figure 5a, c). Once again, the peptide does not form a hydrophobic core. Since this peptide is very short, the molecule can not be described by a single well-determined structure. It can be rather characterized by several somewhat similar conformers. In this molecule, only the following three hydrogen bonds are to be assigned: CO(Gln2)-NH(Lys4), CO(Ile5)-NH(Gln8) and CO(Trp6)-NH(Asn9). There are a number of conformer families, the largest one with the lowest residual constraint violations contains 17 structures. The atomic RMSD for the backbone and for all heavy atoms (17 structures being superimposed in the 2–11 region) is 0.36 ± 0.17 and 0.83 ± 0.21 Å, respectively.

Analysis of the Torsional Values

Penetratin has a helix-like structure ($\phi \approx -55 \pm 15^\circ$, $\varphi \approx -45 \pm 15^\circ$) in its middle segment, which starts and ends with a β-turn-like structure (Table 7). (6,14-Phe)-penetratin has an elongated helical region, slightly twisted in the middle. The dihedral angles suggest that the central part of peptide 3 includes a short helical fragment. Since the latter peptide is very short, the molecule is very flexible. This peptide can easily form β-turns both at the beginning and at the end of its chain. In order to support these statements, average ϕ and φ values were calculated throughout these peptides. Average ϕ and φ values were also calculated for specific parts

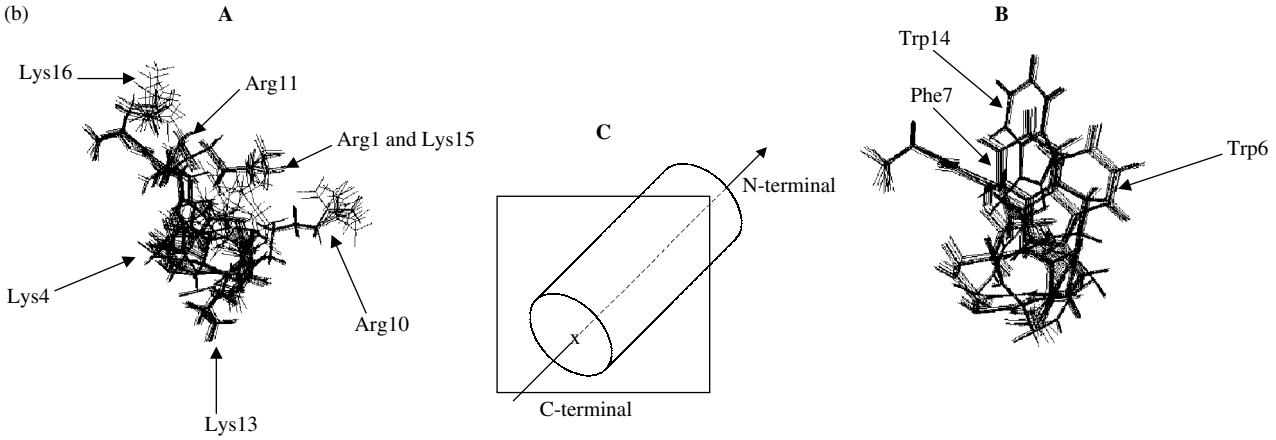

Figure 2 (b) The best 10 structures of penetratin from the plane of the helix, superimposed on the heavy atoms of residues 1–16 in TFE/water = 9 : 1 system. The packing of basic side chains (A), and the aromatic side chains (B), the approximate orientation of the helical cylinder (C).

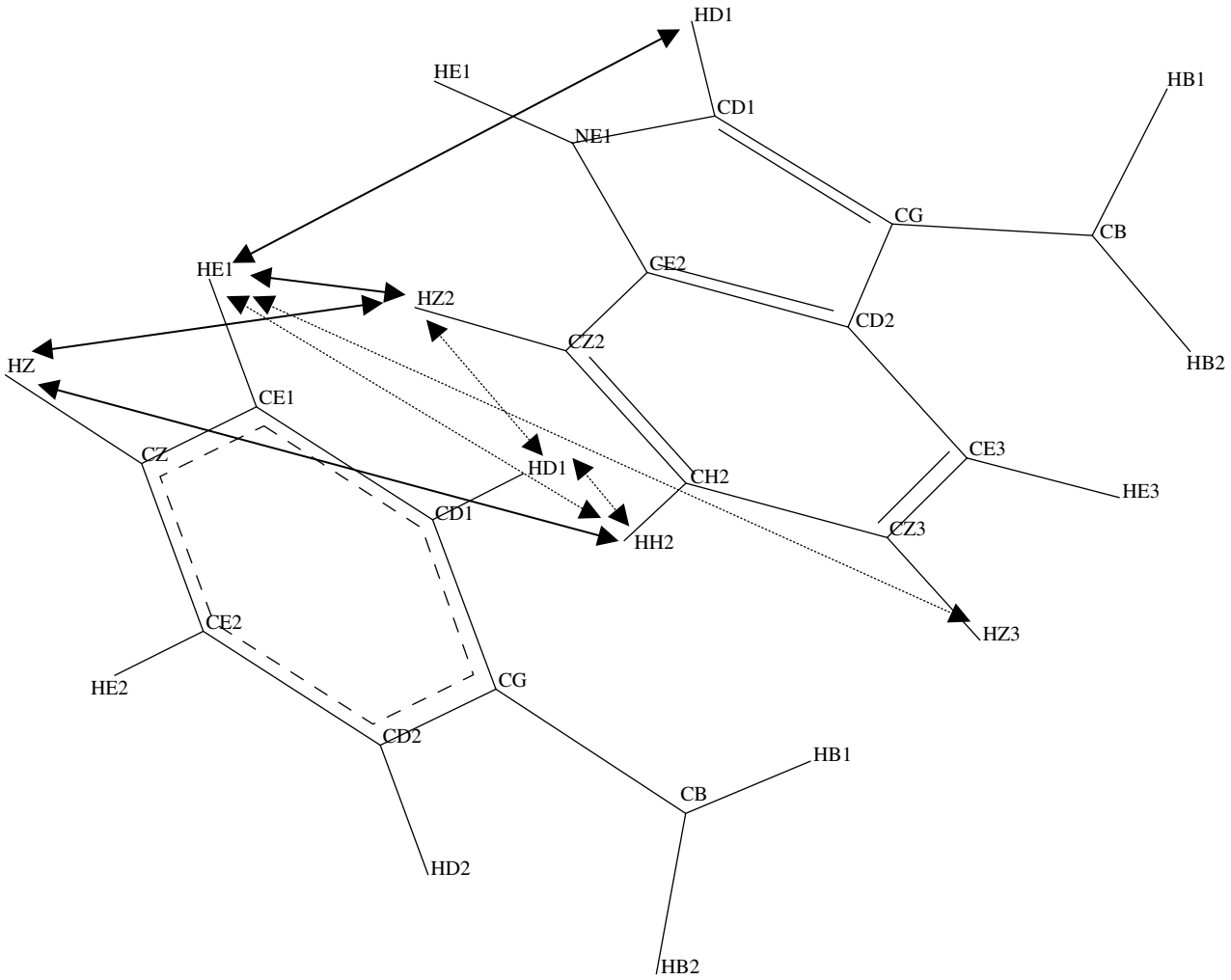

Figure 3 Distances between the aromatic ring of Trp(6) and the Phe(7) in the penetratin as computed based on NMR restraints reported in Table 5.

Table 7 Dihedral Angles[a] and Derived Values of Penetratin and Two of its Derivatives

Penetratin			6,14-Phe-penetratin			Peptide 3		
Amino acid	ϕ[b]	φ	Amino acid	ϕ	φ	Amino acid	ϕ	φ
1		−164.9	1		−33.5	1		−29.7
2	−126.8	−152.6	2	−149.4	−59.3	2	−62	−42.4
3	69.3	37.8	3	−38.4	−46.4	3	39	41.2
4	−115.2	−48.1	4	−72	−39.2	4	−116.3	−45.5
5	−121.6	−12.3	5	−53.7	−28.8	5	−72.7	−34.2
6	−41.2	−98.2	6	−75.6	−33	6	−63.2	−57.3
7	−56.9	−9.4	7	−92	−51.6	7	−50.6	−20
8	−72.3	−35.7	8	−44.3	−33.3	8	−91.1	
9	−74.4	−22.4	9	−59.9	−9.1	9		
10	−93.1	−15.6	10	−130.9	1.5	10		−15.4
11	−81.5	−45.4	11	−113.7	−51.7	11	−93.7	
12	−50.7	−30.3	12	−84.5	−36.1	12		
13	−78.5	45.4	13	−72.2	−14	13		−70.6
14	−113.4	−165.3	14	−77.1	−15.7	14	−86.4	−112.3
15	−127.2	13.5	15	−139.9	7.6	15	−159.1	39
16	47.8		16	−53.6		16	−34.1	
	Average[c]			Average			Average	
	ϕ	φ		ϕ	φ		ϕ	φ
All residues	−69	−46.9	All residues	−83.8	−29.5	All residues	−71.8	−31.6
From 4 to 12	−78.5	−35.3	From 3 to 14	−76.2	−29.8	From 3 to 10	−66.9	−39.3
From 6 to 12	−67.2	−36.7	From 12 to 14	−77.9	−21.9	From 4 to 9	−76.3	−51.6
From 7 to 12	−71.5	−26.5	From 3 to 9	−62.3	−34.5	From 5 to 8	−69.4	−31.7
	Standard deviation[d]			Standard deviation			Standard deviation	
	ϕ	φ		ϕ	φ		ϕ	φ
All residues	58.8	68.5	All residues	34.9	19.9	All residues	50	44.4
From 4 to 12	27.6	27.4	From 3 to 14	26.9	17.2	From 3 to 10	47.3	44.9
From 6 to 12	18.3	29.7	From 12 to 14	6.2	12.3	From 4 to 9	23.7	21.5
From 7 to 12	15.6	13.3	From 3 to 9	18.8	13.8	From 5 to 8	17.1	18.8

[a] Structures were calculated by XPLOR 3.851. Dihedral angles were derived from the mean structure computed for $TFEd_2$/water = 9 : 1 system at 298 K.
[b] All values in degree.
[c] Average = $\frac{1}{n}\sum_{i=1}^{n} x_i$, $x_i = \phi$ or φ, n = number of elements.
[d] Standard deviation = $\sqrt{\frac{n\sum x^2 - \left(\sum x\right)^2}{n(n-1)}}$, $x = \phi$ or φ, n = number of elements.

of the peptides, with standard deviations in all cases. Analysis of the locations of dihedral angle in these peptides on the Ramachandran surface revealed that they fall within the helical region. This supports the results of CD deconvolution; the helical conformation is a substantial component of these structures in TFE/water = 9 : 1. Since the standard deviation of the dihedral angles for the whole molecules is considerable (over 30°), as expected, we examined which parts of the molecules are helical. The dihedral angle data are in keeping with the CD deconvolution; the largest helical content is found in (6,14-Phe)-penetratin, where both the 3–9 and the 12–14 regions adopt a helical conformation. In this case, the standard deviations are between 6.2° and 18.8°. In penetratin only the 7–12 region (standard deviations of 15.6° for ϕ and 13.3° for φ) and in peptide 3 only the 5–8 region (standard deviations of 17.1° for ϕ and 18.8° for φ) exhibit a helical character. Since these standard deviations are relatively large, these regions must be regarded as non-ideal helical regions. The ratios of these segments correspond to the ratios derived from CD data, analysed by the CCA+ method.

Table 8 Dihedral Angles of Penetratin[a] and the Third Helix of Antennapedia Homeodomain

	Penetratin			Homeodomain		
	ϕ[b]	ψ	χ^1	ϕ	ψ	χ^1
Arg1	—	−164.9	55.5	−60.2	−52.1	−170.0
Gln2	−126.8	−152.6	−57.4	−72.7	−29.3	83.6
Ile3	69.3	37.8	−83.8	−63.6	−45.7	−65.9
Lys4	−115.2	−48.1	4.7	−52.4	−50.4	179.7
Ile5	−121.6	−12.3	58.7	−57.5	−52.3	−90.4
Trp6	−41.2	−98.2	59.6	−62.7	−44.5	−169.2
Phe7	−56.9	−9.4	78.5	−64.0	−44.1	−91.9
Gln8	−72.3	−35.7	32.0	−56.0	−48.4	178.3
Asn9	−74.4	−22.4	−87.6	−58.2	−47.0	−82.9
Arg10	−93.1	−15.6	103.8	−64.5	−30.8	−115.9
Arg11	−81.5	−45.4	−138.9	−93.7	−22.2	62.5
Met12	−50.7	−30.3	72.2	−56.3	142.3	136.7
Lys13	−78.5	45.4	−50.3	74.6	−3.1	−159.5
Trp14	−113.4	−165.3	−110.8	−106.1	−73.9	−152.8
Lys15	−127.2	13.5	24.7	−75.5	16.8	−58.9
Lys16	−47.8	—	−63.0	−136.4	12.3	−82.0

[a] Dihedral angles of penetratin were derived from the mean structure measured in $TFEd_2$/water = 9 : 1 system at 298 K. The dihedral angles of homeodomain are reported [2].
[b] All values in degree.

CD Data Measurement and Deconvolution

CD spectroscopy sensitively reflects conformational changes in molecules. For linear peptides, such effects can, in general, be recorded when alterations are made in the polarity of the molecular environment. The dielectric constant of the TFE/water solvent mixture varies from a low (26.3) to a higher (78.4) value. For the three penetratin models, a total of 21 CD curves (because of solubility problems some spectra are missing) were acquired at TFE/water ratios of 0%, 10%, 25%, 50%, 75%, 90%, 94% and 100% (Figures 6–8, Table 9). The curves are similar to those results described earlier in water, water/hexafluoroisopropanol and 10 mM SDS solution [12]. At high TFE concentrations (an environment of low polarity), all three models gave a class C-type CD spectrum [24,25] referring to β-turns (type I or III) and/or α- (or 3_{10})-helices. In contrast, at high water concentration (a polar medium), U-type CD spectra [26] were recorded for all three models. The qualitative spectral features of these model peptides at intermediate TFE/water ratios can be described as mixtures of class U and C-type CD curves. How ever, there are more, than a single isobestic points on the curves acquired at different TFE/water ratios, therefore the curves consist of more than two components. Quantitative CD spectra analysis was performed with the Convex Constraint Analysis program (CCA+) developed in our laboratory [18,19] (I. Jakli and A. Perczel,unpublished results). This method operates on a set of spectra (21 CD curves in this case), providing both pure CD component curves (called pure components) and coefficients or weight factors.

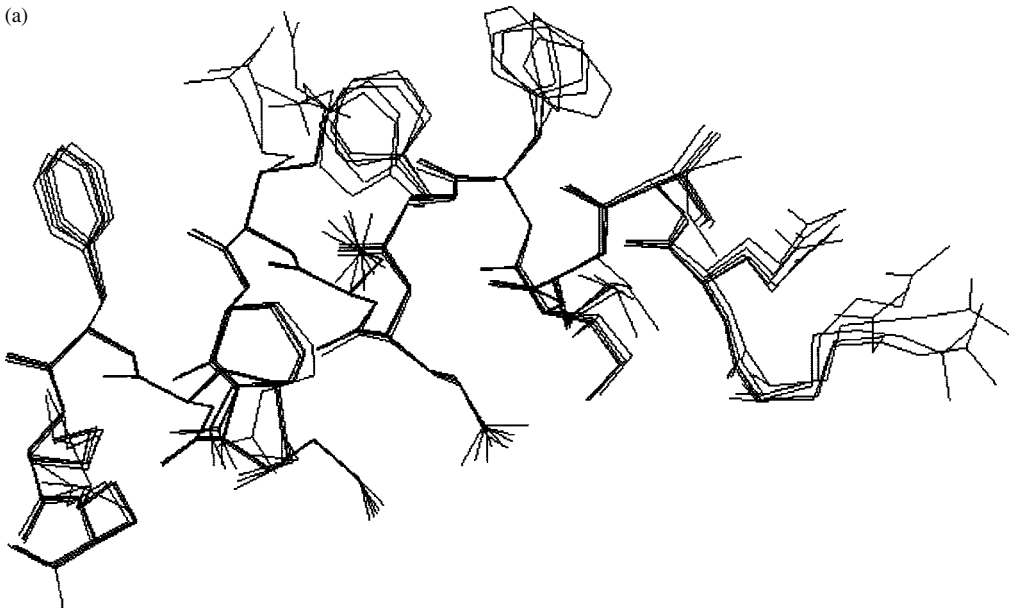

Figure 4 (a) The best 5 structures of (6,14-Phe)-penetratin, superimposed on the heavy atoms of residues 1–16.

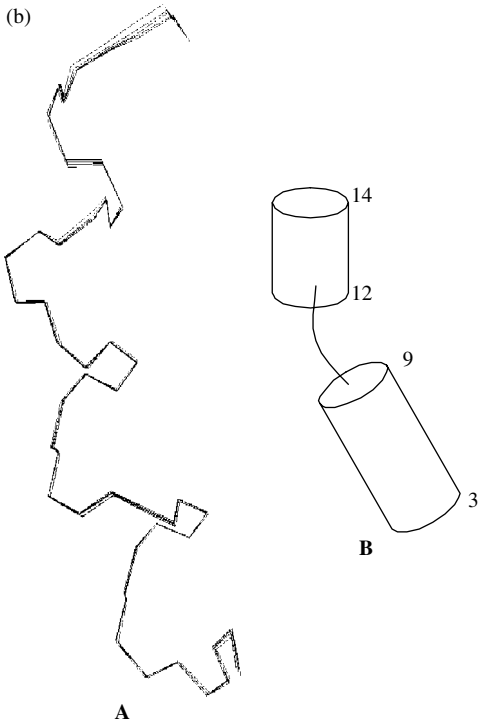

Figure 4 (b) The 5 best backbone structures of (6,14-Phe)-penetratin, superimposed on the heavy atoms of residues 1–16 (A), The two helical segments are shown schematically (B).

The results obtained for three pure components (Figure 9) are straightforward to interpret. The first pure component (dashed line) shows features similar to those of class C-type spectra, with relatively low spectral intensities typically assigned to type I (or III) β-turn(s). The second pure component with an $n\pi^*$ transition ($\approx$224 nm) and with a $\pi\pi^*$ exciton couplet ($\approx$197/210 nm), is typical of α-helices. The third component is a U-type CD curve (intensive negative maximum below 200 nm), which is often associated with polyproline II type structures and/or with atypical (random) conformers. Conformational weights (Table 10 and Figure 10) coupled with these pure component curves are used to reconstruct the experimental CD curves. In this case, this can be done with very low residual error.

For all three peptide models, an increase of the TFE ratio relative to water, clearly increases the helical and/or β-turn content and decreases the atypical or random part of the backbone conformation (Table 10 and Figure 9). In pure TFE, the structures of both penetratin and peptide 3 appear to be assemblies of type I and III β-turns, while the conformation of (6,14-Phe)-penetratin is more like that of an α-helix.

NMR spectroscopy indicates that in a predominantly aqueous medium the structure of penetratin can be described only in terms of several different conformers. The mainly U-type CD spectrum for this peptide moiety in pure water agrees with the above NMR conclusions. Thus, the CD spectra of penetratin and peptide 3 (Figures 6 and 8) reveal similar conformational behaviour. Surprisingly, the proportion of the type I (or III) β-turn is constantly higher than that of the α-helix, exceeding 70% for both peptides in a highly apolar medium. We presume that isolated and/or cumulated β-turn segments can easily be formed in both of these molecules. It should be mentioned that the

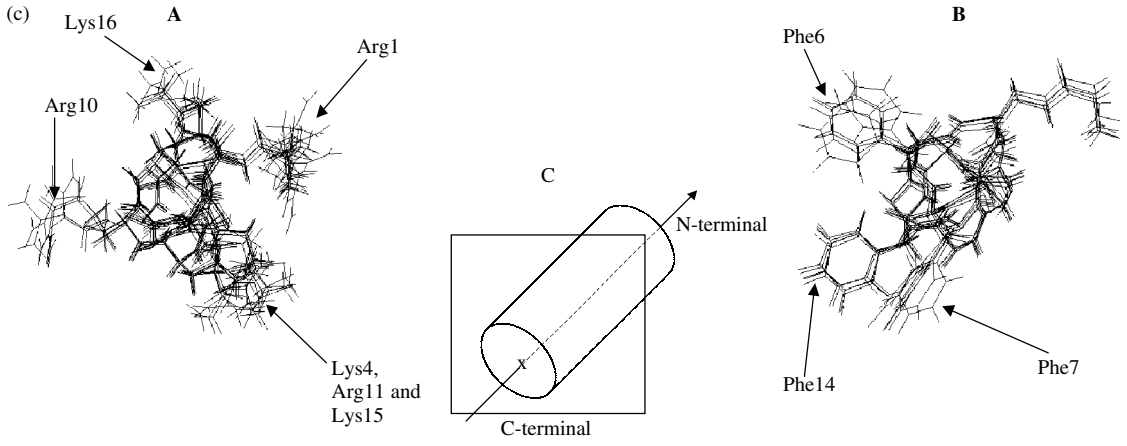

Figure 4 (c) The best 5 structures of (6,14-Phe)-penetratin from the plane of the helix, superimposed on the heavy atoms of residues 1–16. The packing of basic side chains (A) is on the left, and the aromatic side chains (B) is on the right, the approximate orientation of the helical cylinder (C) is in the middle.

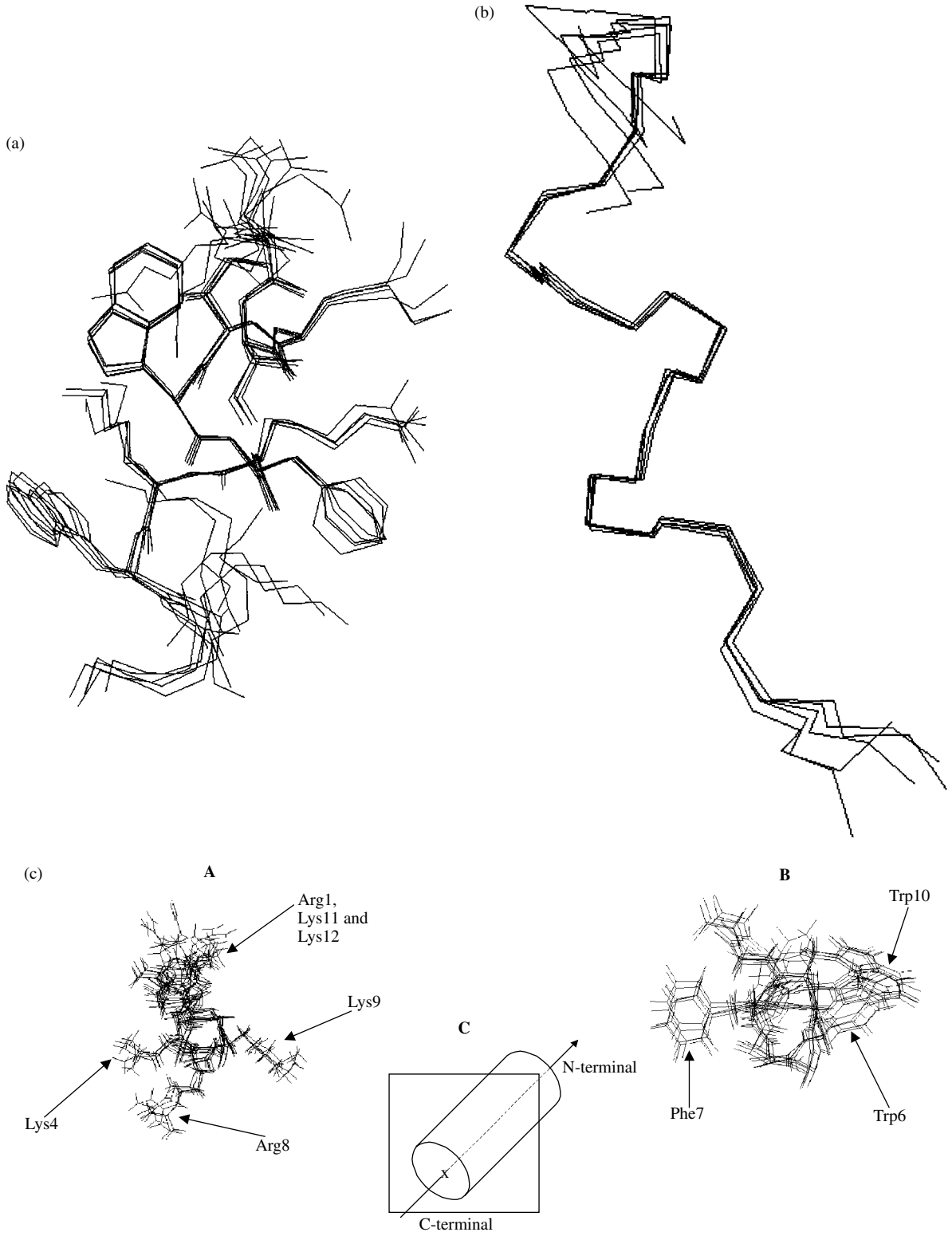

Figure 5 (a) The best 5 structures of peptide 3, superimposed on the heavy atoms of residues 1–12. (b) The 5 best backbone structures of peptide 3, superimposed on the heavy atoms of residues 1–12. (c) The best 5 structures of peptide 3 from the plane of the helix, superimposed on the heavy atoms of residues 1–12. The packing of basic side chains (A) is on the left, and the aromatic side chains (B) is on the right, the approximate orientation of the helical cylinder (C) is in the middle.

Table 9 Data of Circular Dichroism Spectra

TFE[a] (%)	Penetratin			(6.14-Phe)-penetratin			Peptide 3		
	Maximum of $\pi \rightarrow \pi^*$	Negative maximum of $\pi \rightarrow \pi^*$	Negative maximum of $n \rightarrow \pi^*$	Maximum of $\pi \rightarrow \pi^*$	Negative maximum of $\pi \rightarrow \pi^*$	Negative maximum of $n \rightarrow \pi^*$	Maximum of $\pi \rightarrow \pi^*$	Negative maximum of $\pi \rightarrow \pi^*$	Negative maximum of $n \rightarrow \pi^*$
0	—	−1.625 (197.7)	0.071 (227.4)	—	−2.436 (195.2)	0.124 (220.4)	—	−2.167 (198.5)	0.201 (227.0)
10	—	—	—	—	−1.914 (198.1)	0 (220.0)	—	− 2.191 (199.1)	0.264 (227.2)
25	—	−1.01 (202.2)	−0.435 (217.1)	0.368 (193.5)	−1.143 (204.4)	−0.561 (225.6)	0.189 (186.3)	−1.565 (201.3)	−0.133 (231.7)
50	0.883 (188.6)	−0.933 (204.2)	−0.561 (219.3)	2.688 (193.5)	−1.328 (207.1)	−1.053 (223.1)	0.991 (188.3)	−1.431 (204.3)	—
75	1.433 (190.3)	−1.085 (206.6)	−0.823 (217.2)	4.943 (193.3)	−1.831 (207.6)	−1.636 (221.7)	1.860 (190.5)	−1.577 (205.6)	−0.726 (226.8)
90	—	—	—	8.155 (193.2)	−2.695 (207.9)	−2.305 (221.6)	3.127 (191.0)	−1.876 (206.5)	−1.084 (222.6)
100	3.162 (191.1)	−1.760 (207.7)	−1.353 (220.1)	8.098 (193.2)	−2.879 (209.1)	−2.642 (221.3)	4.554 (192.3)	−2.389 (206.3)	−1.365 (222.9)

[a] Spectra were recorded in TFE/water systems at 298 K. $\Delta\varepsilon$[$dm^3\ mol^{-1}\ cm^{-1}$], and λ [nm] (in brackets) values are provided.

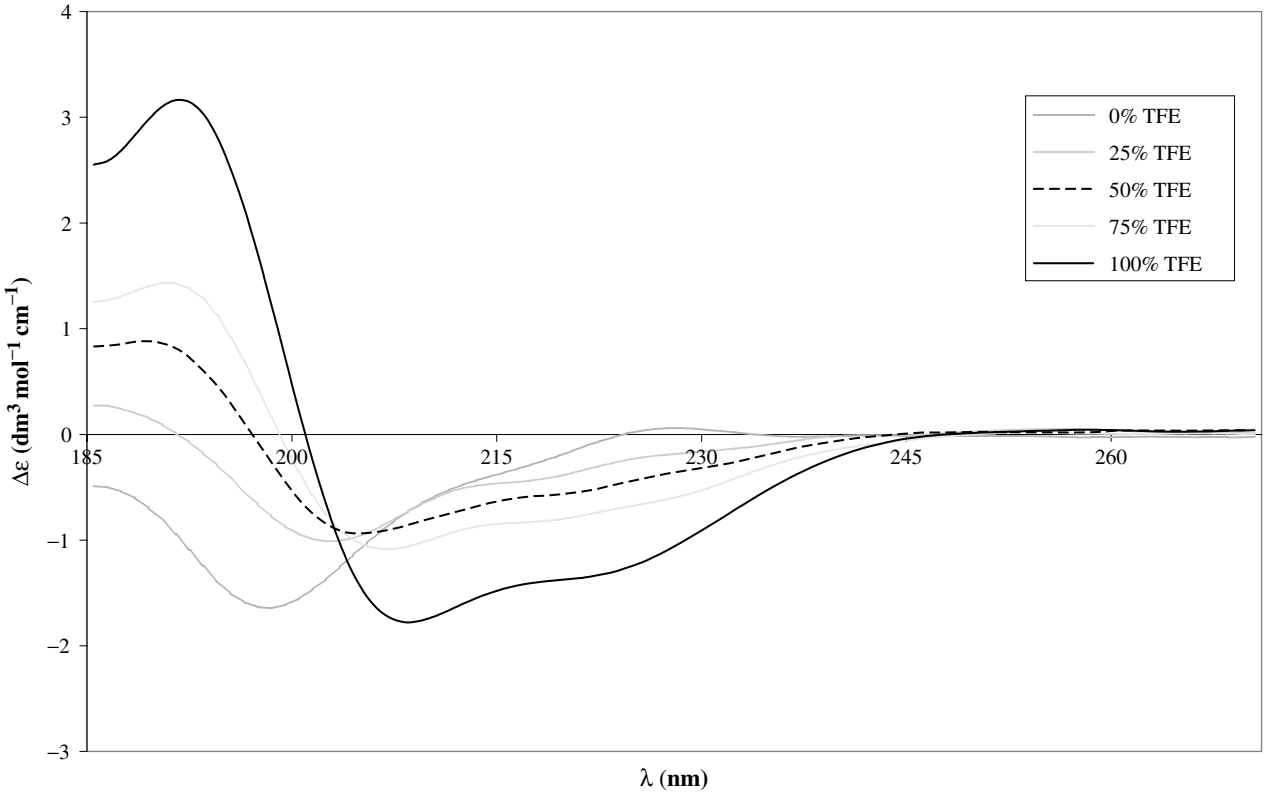

Figure 6 CD spectra of penetratin recorded in different TFE/water systems.

differentiation of repeated type I (or III) β-turns from α-helices is very complicated either by CD or by NMR spectroscopy. In both types of secondary structural elements, the adjacent ϕ and ψ values are close to a value of -50° and -40°, respectively. Analysis of the conformational weights (Figure 10) suggests that (6,14-Phe)-penetratin is closer to an ideal α-helix at all TFE ratios than either penetratin or peptide 3. The latter two model systems exhibit conformational features similar to β-turns.

DISCUSSION

The structures of penetratin and its two analogues have been analysed by circular dichroism and ^{1}H-NMR spectroscopy. Raw data were recorded in water/trifluoro-ethanol solvent mixtures. The aqueous solutions simulate the extracellular matrix, while solutions containing high amounts of trifluoroethanol simulate a membrane-like environment. By means of the CCA+ deconvolution method, the CD spectra of these peptides were resolved to three components. The dominant component is the U-type CD curve, characteristic of random conformers in aqueous solutions. For all three peptides, even in 25%, 10% and 0% TFE-containing systems, a low but significant amount of helical proportion was assigned. In the system TFEd_2/water = 1 : 9, the structures of these peptides can not be determined by means of NMR spectroscopy. However, consecutive and relatively strong NH(i)/NH($i+1$) and CHβ(i)/NH($i+1$) NOEs can be found in the NOESY spectra, indicating that ordered local structures are present in all three molecules. This is supported by the significant upfield shifts of the Hα protons relative to the random coil values. We concluded that these peptides form nascent helices in mainly aqueous solution. In the system TFEd_2/water = 9 : 1, both NMR- and CD-spectroscopy indicated that these peptides form helical conformations. The enhancing effect of TFE on peptide helices is not unspecific [27–29]. The addition of TFE to water stabilizes helices only in those regions that have a helical character even in aqueous solution. By means of CD spectroscopy the structural changes can be followed; molecules with a helical character in TFE and in the TFE/water = 9 : 1 system, gradually lose their helical property and adopt a nascent helix-like structure as the water content

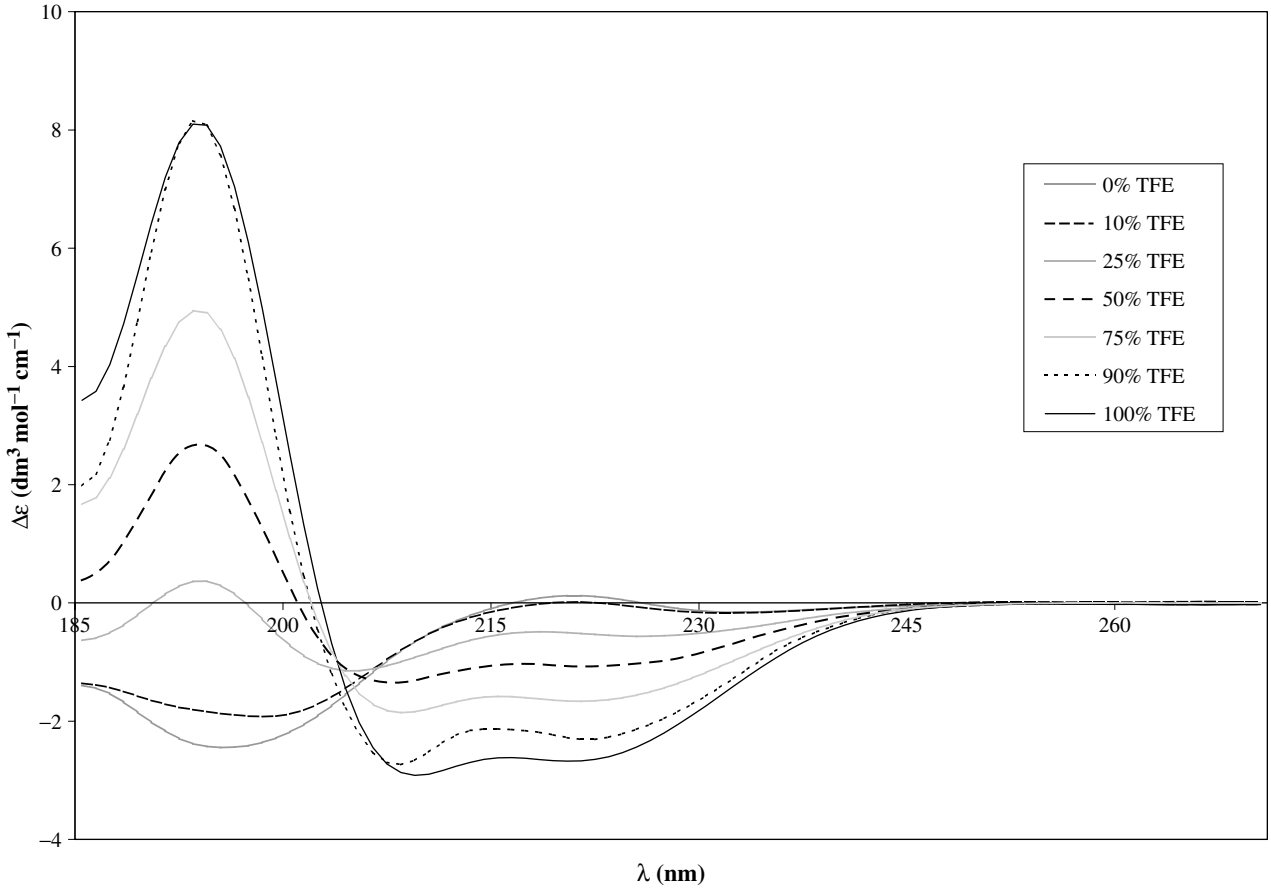

Figure 7 CD spectra of (6,14-Phe)-penetratin recorded in different TFE/water systems.

in the solvent mixture is increased. To check the reversibility of conformational changes a complementary experiment was accomplished as follows: more and more TFE was added stepwise to the solvent-system containing primary water and several CD spectra were recorded. The pair-wise comparison of the relevant CD curves shows great similarity. This indicates that regardless of the way that the solvent-mixture is obtained the peptide conformation is practically identical. Considering this fact, structural regrouping of these peptides as a function of their molecular environment is plausible, and thus may play a decisive role in membrane penetration.

The structures of the three peptides were established at an atomic level to see the effect of mutation. The three-dimensional structure of molecules can only be determined at a high TFE concentration by means of NMR spectroscopy. Each peptide adopts a helical conformation in TFE/water = 9 : 1. Both penetratin and (6,14-Phe)-penetratin contain α-helical and 3_{10}-helical fragments, while the central part of peptide 3 is close to a 3_{10}-helix. Resolution of the CD spectra by the CCA+ deconvolution method proved that the main component is a turn-like (3_{10}-helical) one for penetratin and peptide 3, and an α-helical component for (6,14-Phe)-penetratin. Analysis of the dihedral angles surprisingly revealed that (6,14-Phe)-penetratin contains the longest helical segment (3–12), interrupted by a β-turn. The *N*-terminal end of the segment is rather α-helical, and the *C*-terminal part of the helix resembles a 3_{10}-helix. The structure of this molecule proves that the analogues of penetratin can adopt a helical structure without tryptophans. Penetratin and peptide 3 have helical parts only in the centre of the molecules (6–12 and 5–9), and these segments begin and end with β-turns. The latter two molecules do not form an ideal helical structure, and the turn-like component is therefore the dominant one of the CD spectra. The backbones of the longer molecules are stabilized by multiple hydrogen bonds. In contrast, peptide 3 contains only three hydrogen bonds. We presume that this molecule

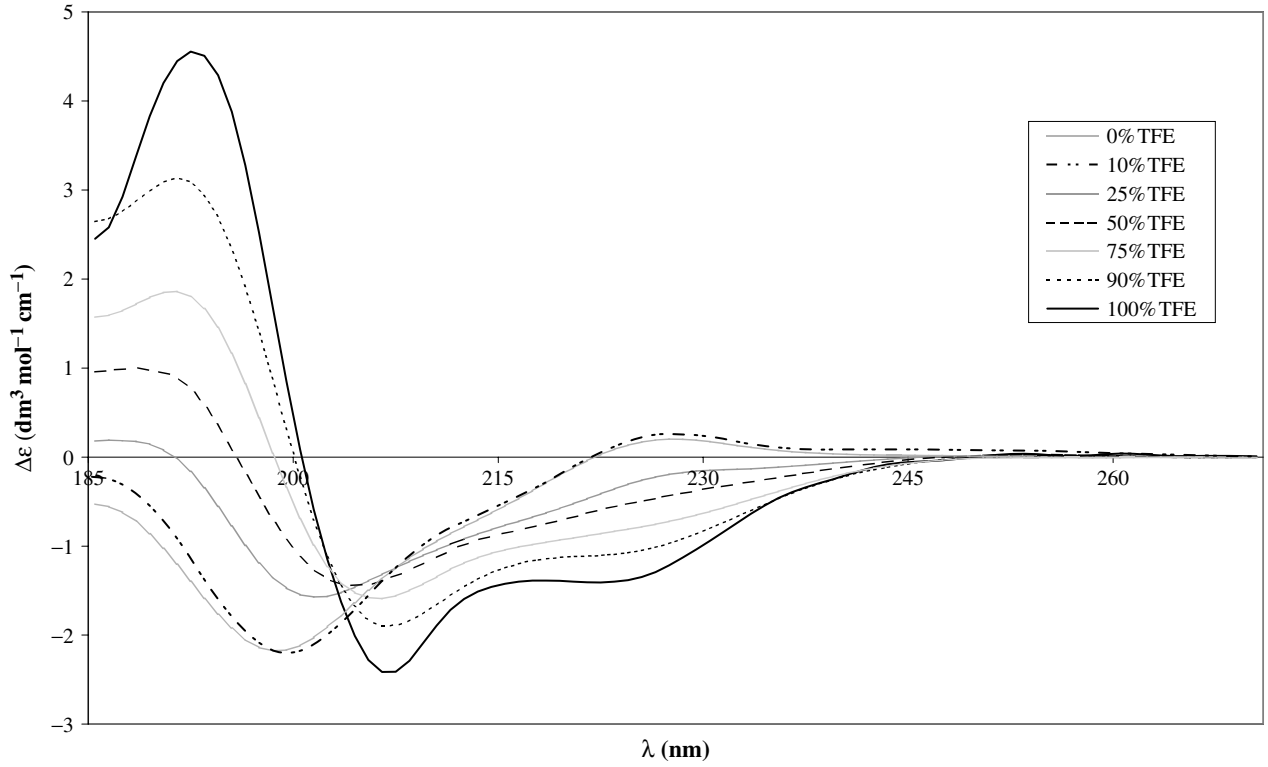

Figure 8 CD spectra of peptide 3 recorded in different TFE/water systems.

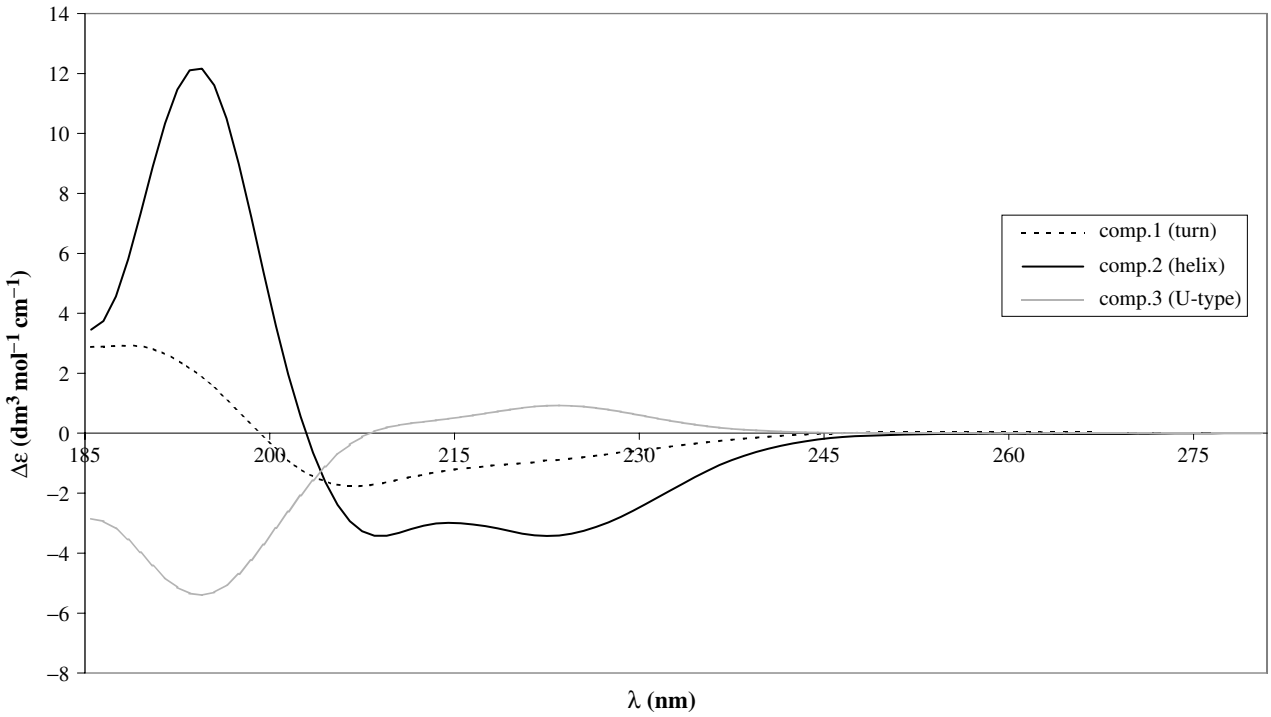

Figure 9 The three pure CD component curves as deconvoluted by CCA+ [19].

Table 10 Relative Ratios (in %) of the Three Pure Components as Deconvoluted by CCA+

	TFE(%)	β-turn	α-(or 3_{10})-helix	RND[a]
Peptide 3	0	40	4	56
	10	50	0	50
	25	46	9	46
	50	57	9	34
	75	62	13	24
	90	82	12	6
	94	87	13	0
	100	68	26	5
(6.14-Phe)-penetratin	0	12	12	76
	10	6	18	76
	25	0	33	67
	50	6	44	50
	75	21	51	28
	90	8	73	20
	94	0	79	21
	100	37	63	0
Penetratin	0	30	11	60
	25	37	14	49
	50	45	15	40
	75	50	17	33
	100	72	18	10

[a] Atypical conformation and/or conformational ensemble.

is not long enough to have one well-determined conformation. Penetratin has a hydrophobic core and the movements of its side chains are therefore restrained. The hydrophobic core can not be found in the two analogue peptides, whose side chains are very flexible. In (6,14-Phe)-penetratin, where both tryptophans are replaced by phenylalanines, the movement of the aromatic side chains is larger than in penetratin. We postulate that phenylalanines of positions 6 and 7 can not interact with each other and therefore this peptide does not form a hydrophobic core. The three peptides have a little different conformation and simultaneously a slightly different translocational activity. We suppose that the complex and still unknown molecular mechanism of penetration itself is not necessarily coupled with a fully helical secondary structure. Nevertheless, the fact that all three molecules can penetrate into the cell and they all adopt partially helical structure is a conclusive observation.

Acknowledgements

The authors thank Professor. M. Hollósi and Dr P. Forgó for helpful discussions concerning various aspects of this work.

This research was supported in part by grants from the Hungarian Scientific Research Fund (OTKA T030841, OTKA T032486 and AKP 98-89 2,4).

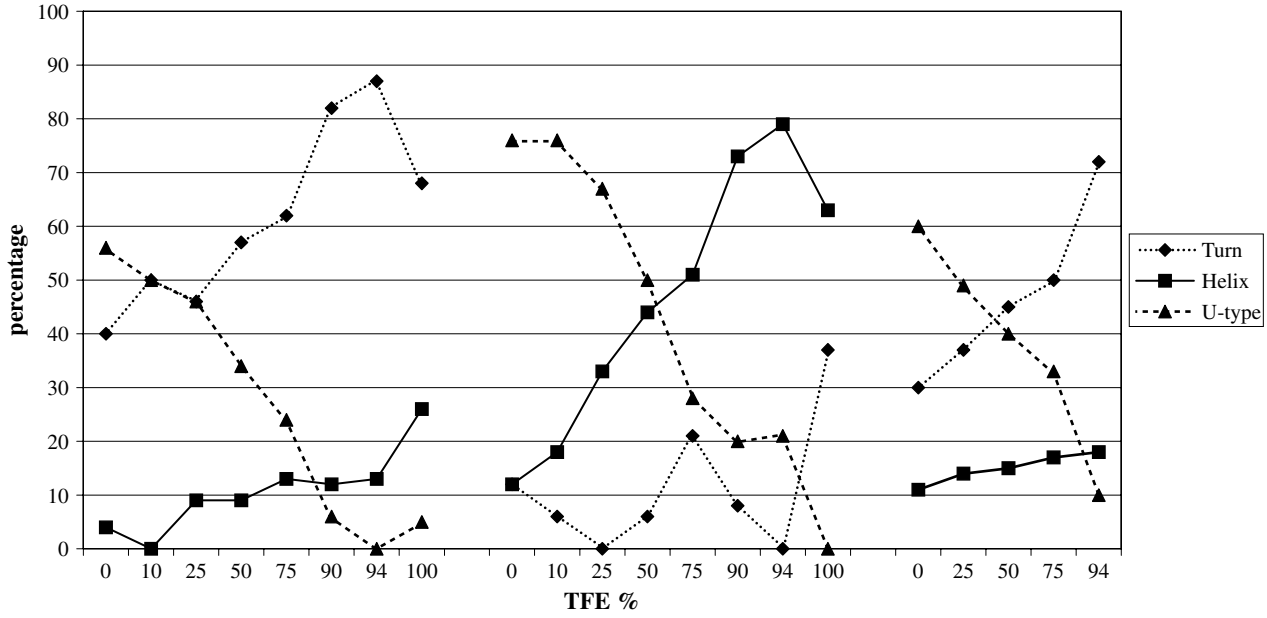

Figure 10 The percentage of the three pure components in the penetratin-peptides recorded in different TFE/water systems. peptide 3 is on the left, penetratin is on the right, and (6,14-Phe)-penetratin is in the middle.

Special thanks to Accelrys, for their NMR software-package.

REFERENCES

1. Gehring WJ. Homeo boxes in the study of development. *Science* 1987; **236**: 1245–1252.
2. Qian YQ, Billeter M, Otting G, Müller M, Gehring WJ, Wüthrich K. The structure of the Antennapedia homeodomain determined by NMR spectroscopy in solution: comparison with prokaryotic repressors. *Cell* 1989; **59**: 573–580.
3. Qian YQ, Otting G, Furukubo-Tokunaga K, Affolter M, Gehring WJ, Wüthrich K. NMR structure determination reveals that the homeodomain is connected through a flexible linker to the main body in the *Drosophila* Antennapedia protein. *Proc. Natl. Acad. Sci. USA* 1992; **89**: 10 738–10 742.
4. Qian YQ, Otting G, Billeter M, Müller M, Gehring WJ, Wüthrich K. Nuclear magnetic resonance spectroscopy of a DNA complex with the uniformly ^{13}C-labeled Antennapedia homeodomain and structure determination of the DNA-bound homeodomain. *J. Mol. Biol.* 1993; **234**: 1070–1083.
5. Le Roux I, Joliot AH, Bloch-Gallego E, Prochiantz A, Volovitch M. Neurotrophic activity of Antennapedia homeodomain depends on its specific DNA-binding properties. *Proc. Natl. Acad. Sci. USA* 1993; **90**: 9120–9124.
6. Derossi D, Joliot AH, Chassaign G, Prochiantz A. The third helix of the Antennapedia homeodomain translocates through biological membranes. *J. Biol. Chem.* 1994; **269**: 10 444–10 450.
7. Derossi D, Calvet S, Trembleau A, Brunissen A, Chassaign G, Prochiantz A. Cell internalization of the third helix of the Antennapedia is receptor-independent. *J. Biol. Chem.* 1996; **271**: 18188–18193.
8. Thoren EG, Persson D, Karlsson M, Norden B. The Antennapedia peptide penetratin translocates across lipid bilayers — the first direct observation. *FEBS Lett.* 2000; **482**: 265–268.
9. Theodore L, Derossi D, Chassaign G, Llirbat B, Kubes M, Jordan P, Chneiweis H, Godement P, Prochiantz A. Intraneuronal delivery of protein kinase C pseudosubstrate leads to growth cone collapse. *J. Neurosci.* 1996; **15**: 7158–7167.
10. Troy CM, Derossi D, Prochiantz A, Shelanski ML. Down regulation of SOD1 leads to cell death by the NO-peroxy-nitrite pathway. *J. Neurosci.* 1996; **16**: 253–261.
11. Derossi D, Chassaign G, Prochiantz A. Trojan peptides: the penetratin system for intracellular delivery. *Trends in Cell Biol.* 1998; **8**: 84–87.
12. Berlose JP, Convert O, Derossi D, Brunissen A, Chassaign G. Conformational and associative behaviours of the third helix of antennapedia homeodomain in membrane-mimetic environments. *Eur. J. Biochem.* 1996; **242**: 372–386.
13. Waterhous WC, Johnson J. Importance of environment in determining secondary structure in proteins. *Biochemistry* 1994; **33**: 2121–2128.
14. Brünger AT. *X-PLOR Version 3.851*, Yale University Press: New Haven, CT, 1996.
15. Nilges M, Clore GM, Gronenborn AM. Determination of three-dimensional structures of proteins from interproton distance data by dynamical simulated annealing from a random array of atoms. *FEBS Lett.* 1988; **239**: 129–136.
16. Nilges M, Kuszewski J, Brünger AT. In *Computational Aspects of the Study of Biological Macromolecules by NMR*, Hoch JC (ed.). Plenum Press: New York, 1991.
17. Koradi R, Billeter M, Wüthrich K. MOLMOL: a program for display and analysis of macromolecular structures. *J. Mol. Graph.* 1996; **14**: 51–55.
18. Perczel A, Hollósi M, Tusnády G, Fasman GD. Convex constraint analysis: a natural deconvolution of circular dichroism curves of proteins. *Protein Engineering* 1991; **4**: 669–679.
19. Perczel A, Park K, Fasman GD. Analysis of the circular dichroism spectra of proteins using the convex constraint algorithm: a practical guide. *Anal. Biochem.* 1992; **203**: 83–93.
20. Dyson HJ, Rance M, Houghten RA, Wright PE, Lerner RA. Folding of immunogenic peptide fragments of proteins in water solution II. The nascent helix. *J. Mol. Biol.* 1988; **201**: 201–217.
21. Wishart DS, Sykes BD, Richards FM. The chemical shift index: a fast and simple method for the assignment of protein secondary structure through NMR spectroscopy. *Biochemistry* 1992; **31**: 1647–1651.
22. Wishart DS, Bigam CG, Holm A, Hodges RS, Sykes BD. 1 H, 13 C and 15N random coil NMR chemical shifts of the common amino acids. I. Investigations of the nearest-neighbour effects. *J. Biomol. NMR* 1995; **5**: 67–81.
23. Bradley EK, Thomason JF, Cohen FE, Kosen PA, Kuntz ID. Studies of synthetic helical peptides using circular dichroism and nuclear magnetic resonance. *J. Mol. Biol.* 1990; **215**: 607–622.
24. Woody RW. In *Peptides, Polypeptides and Proteins*, Blout ER, Bovey FA, Lotan N, Goodman M (eds). Wiley: New York, 1974; 338–350.
25. Woody RW. In *The Peptides*, Hruby VJ (ed.). Academic Press: New York, 1985; 15–114.
26. Perczel A, Hollósi M. In *Circular Dichroism and the Conformational Analysis of Biomolecules*, Fasman GD (ed.). Plenum Press: New York, 1996; 285–380.
27. Segawa SI, Fukuno T, Fujiwara K, Noda Y. Local structures in unfolded lysozyme and correlation with native conformation: helix-forming or breaking propensity of peptide segments. *Biopolymers* 1991; **31**: 457–509.

28. Blanco FJ, Jimenez MA, Rico M, Santoro J, Herranz J, Nieto JL. The homologous angiogenin and ribonuclease *N*-terminal fragments fold into very similar helices when isolated. *Biochem. Biophys. Res. Commun.* 1992; **182**: 1491–1498.

29. Dyson HJ, Merutka G, Waltho JP, Lerner RA, Wright PE. Folding of peptide fragments comprising the complete sequence of proteins. Models for initiation of protein folding. I. Myohemerythrin.*J. Mol. Biol.* 1992; **226**: 795–817.